Neurochemistry International 131 (2019) 104565

Contents lists available at ScienceDirect

Neurochemistry International

journal homepage: www.elsevier.com/locate/neuint

Histamine H_1 and H_3 receptor activation increases the expression of Glucose Transporter 1 (GLUT-1) in rat cerebro-cortical astrocytes in primary culture

Juan Parra-Abarca[a], Nayeli Rivera-Ramírez[a], Luis-Fernando Villa-Maldonado[a], Ubaldo García-Hernández[a], Penélope Aguilera[b], José-Antonio Arias-Montaño[a,*]

[a] *Departamento de Fisiología, Biofísica y Neurociencias, Centro de Investigación y de Estudios Avanzados del IPN, Av. IPN 2508, Zacatenco, 07360, Ciudad de México, Mexico*

[b] *Laboratorio de Patología Vascular Cerebral, Instituto Nacional de Neurología y Neurocirugía Manuel Velasco Suárez, Insurgentes Sur 3877, La Fama, 14269, Ciudad de México, Mexico*

ARTICLE INFO

Keywords:
Histamine
GLUT-1
Astrocytes
Histamine H_1 receptor
Histamine H_3 receptor
Glucose transport

ABSTRACT

Astrocytes take up glucose via the 45 kDa isoform of the Glucose Transporter 1 (GLUT-1), and in this work we have investigated whether histamine regulates GLUT-1 expression in rat cerebro-cortical astrocytes in primary culture. Cultured astrocytes expressed histamine H_1 and H_3 receptors (H_1Rs and H_3Rs) as evaluated by radioligand binding. Receptor functionality was confirmed by the increase in the intracellular concentration of Ca^{2+} (H_1R) and the inhibition of forskolin-induced cAMP accumulation (H_3R). Quantitative RT-PCR showed that histamine and selective H_1R and H_3R agonists (1 h incubation) significantly increased GLUT-1 mRNA to 153 ± 7, 163 ± 2 and 168 ± 13% of control values, respectively. In immunoblot assays, incubation (3 h) with histamine or H_1R and H_3R agonists increased GLUT-1 protein levels to 224 ± 12, 305 ± 11 and 193 ± 13% of control values, respectively, an action confirmed by inmunocytochemistry. The effects of H_1R and H_3R agonists were blocked by the selective antagonists mepyramine (H_1R) and clobenpropit (H_3R). The pharmacological inhibition of protein kinase C (PKC) prevented the increase in GLUT-1 protein induced by either H_1R or H_3R activation. Furthermore, histamine increased ERK-1/2 phosphorylation, and the effect of H_1R and H_3R activation on GLUT-1 protein levels was reduced or prevented, respectively, by MEK-1/2 inhibition. These results indicate that by activating H_1Rs and H_3Rs histamine regulates the expression of GLUT-1 by astrocytes. The effect appears to involve the phospholipase C (PLC) → diacylglycerol (DAG)/Ca^{2+}→ PKC and PLC → DAG/Ca^{2+} → PKC → MAPK pathways.

1. Introduction

Histamine is a biogenic amine with an important role as chemical transmitter in the gastrointestinal, vascular, immune and nervous systems, and exerts its actions via the activation of four G protein-coupled receptors (H_1 to H_4) identified to date (Haas et al., 2008; Panula et al., 2015). In the central nervous system, histamine participates in a variety of homeostatic functions, including the regulation of appetite and blood glucose levels (Haas et al., 2008; Sim et al., 2014; Pini et al., 2016).

In the mammalian brain, astrocytes constitute the principal structural and trophic supportive elements, and their arranging is critical for the organization of the neurovascular unit that interposes them between blood vessels and neurons (Araque et al., 2001; Fellin and Carmignoto, 2004). This situation reflects the major role of astrocytes in the distribution and metabolism of glucose, necessary to maintain an adequate cerebral activity (Nehlig and Coles, 2007; Duelli and Kuschinsky, 2001; Prebil et al., 2011).

Astrocytes are the main source of glycogen in the brain and take up large amounts of glucose, ~40% of which is destined to glycogen synthesis (Prebil et al., 2011; Hutchinson et al., 2011). Astrocytic glucose uptake is performed by the 45 kDa isoform of the facilitative glucose transporter 1 (GLUT-1), with high capacity of transport and whose expression and activity are modulated by extra and intracellular signals (Augustin, 2010; Maher et al., 1994; Yu and Ding, 1998; Carruthers et al., 2009).

Astrocytes in culture obtained from different regions of the brain

---

Abbreviations: GLUT-1, glucose transporter 1; H_1R, histamine H_1 receptor; H_3R, histamine H_3 receptor; HA, histamine; GFAP, Glial Fibrillary Acid Protein; MAPKs, mitogen-activated protein kinases; PEA, 2-pyridyl-ethylamine; PKC, protein kinase C; PLC, phospholipase C

[*] Corresponding author. Departamento de Fisiología, Biofísica y Neurociencias, Cinvestav-IPN, Av. IPN 2508, Zacatenco, 07360, México, D.F, Mexico.
E-mail address: jaarias@fisio.cinvestav.mx (J.-A. Arias-Montaño).

https://doi.org/10.1016/j.neuint.2019.104565
Received 15 February 2019; Received in revised form 11 September 2019; Accepted 2 October 2019

express H_1, H_2, and H_3 receptors to varying extent (Lipnik-Štangelj and Čarman-Kržan, 2004; Mele and Jurič, 2013), and the activation of H_1 and H_2 receptors increases glycogenolysis in rat astrocytes in primary culture (Arbones et al., 1990).

In some cell types, increased glucose uptake depends on *de novo* synthesis of GLUT-1 protein and its posterior translocation to the plasma membrane (Carruthers et al., 2009). However, to the best of our knowledge whether histamine regulates GLUT-1 transporter expression by astrocytes was unknown. Therefore, in the present study we examined the effect of histamine on GLUT-1 expression by rat cerebrocortical astrocytes in primary culture. We show that histamine increases GLUT-1 mRNA and protein levels via the activation of H_1 and H_3 receptors, and that the effect on GLUT-1 protein levels involves the activation of protein kinase C (PKC) and mitogen-activated protein kinases (MAPKs).

2. Material and methods

2.1. Primary culture of astrocytes from rat cerebral cortex

Cultures were prepared from the brain of neonatal Wistar rats (postnatal days 2–7). All procedures were approved by the Cinvestav Animal Care Committee and followed the guidelines for the care and use of laboratory animals issued by the National Institutes of Health (NIH Publications No. 8023, revised 1978) and the Mexican Council for Animal Care (NOM-062-ZOO-1999). All efforts were made to minimize animal suffering and to use only as many animals were required for proper statistical analysis.

Animals were decapitated and the brain was removed under aseptic conditions. The meninges were retired and the brain was immersed in ice-cold sterile phosphate-buffered saline solution (PBS). Under sterile conditions, cortices were dissected, minced with scissors and the resulting pieces transferred to a Falcon tube (15 ml) containing 3 ml ice-cold sterile Hank's balanced saline solution (HBSS; composition in mM: NaCl 138, $NaHCO_3$ 4.16, $CaCl_2$ 1.26, KCl 5.33, KH_2PO_4 0.44, $MgCl_2$ 0.5, $MgSO_4$ 0.41, Na_2HPO_4 0.3, glucose 5.6, phenol red 0.03). The tissue from 2 animals was rinsed with this solution and then transferred to a siliconized flask containing a mixture of 500 µl trypsin/EDTA solution (0.25%/0.5 mM) and 5 ml sterile DMEM/F12 medium (Dulbecco's modified Eagle's medium/nutrient mixture F12; Gibco, Thermo Scientific, Walthman, MA). After 15 min at 37 °C, the trypsin action was terminated by adding 3 ml sterile DMEM/F12 medium, supplemented with 10% fetal bovine serum (FBS), 0.01 mg/ml streptomycin, 100 U/ml penicillin and 2.5 mM glutamine (Glutamax; Gibco).

The treated tissue was then dissociated by passage (15 times) through a siliconized Pasteur pipette, and the resulting suspension was centrifuged at 300 × *g* for 5 min. The pellet was resuspended in 4 ml sterile DMEM/F12 medium containing FBS, antibiotics, glutamine, 36 µg/ml hydrocortisone and 52 µg/ml sodium selenite. Aliquots (2 ml) of the suspension were placed in glass Petri dishes (100 mm diameter) previously treated for 1 h with poly-L-Lysine (1 mg/10 ml; 100 µl/cm^2), and 4 ml supplemented medium were added. Cells were incubated at 37 °C in a CO_2 incubator (5% CO_2 in air), the medium was replaced by fresh supplemented medium 24 h later, and thereafter every 48 h half the volume was replaced by fresh supplemented medium until cells reached confluence. Immunodetection of the Glial Fibrillary Acid Protein (GFAP; Supplementary Figure 1) showed that 95.0 ± 0.6% of cells were immunoreactive to GFAP in 3 determinations. Supplementary Figure 2 shows that the astrocyte-enriched cultures contained a low number of cells immunoreactive to the microglia marker CD11b/c (OX42) or the oligodendrocyte marker O4 (see Table 1 for a list of the antibodies employed in this study).

2.2. Radioligand binding to cell membranes

Cells, grown in glass Petri dishes, were scrapped in ice-cold lysis buffer (10 mM Tris-HCl, 1 mM EGTA, pH 7.4). Lysates were centrifuged (32,000 × *g*, 20 min at 4 °C) and the pellets (total membranes) were resuspended in incubation buffer. Aliquots of the membrane suspension (~20 µg of protein, bicinchoninic acid assay, BCA, Thermo Scientific, Waltham, MA) were incubated for 1 h at 30 °C in incubation solution containing the corresponding radioligand (H_1 receptors, H_1Rs, 10 nM [^{3}H]-mepyramine; H_3 receptors, H_3Rs, 4 nM [^{3}H]-N-α-methylhistamine, [^{3}H]-NMHA; H_4 receptors, H_4Rs, 14 nM [^{3}H]-histamine). The composition of the incubation buffer (pH 7.4) was: [^{3}H]-mepyramine and [^{3}H]-histamine, 50 mM Tris-HCl; [^{3}H]-NMHA, 50 mM Tris-HCl and 5 mM $MgCl_2$.

The reaction was terminated by adding 1 ml ice-cold Tris-HCl buffer (50 mM, pH 7.4) and samples were filtered through Whatman GF/B glass-fiber paper, presoaked in 0.3% polyethylenimine for 2 h, using a cell harvester (Brandel, Gaithersburg, MD). Filters were washed 3 times with 1 ml ice-cold buffer and then transferred to vials containing scintillator and allowed to stand at room temperature for at least 2 h before the retained radioactivity was determined by liquid scintillation counting (Beckman Coulter LS 6500, Beckman, Brea, CA). Nonspecific binding was determined in parallel incubations with unlabeled ligands (H_1R, 1 µM mepyramine; H_3R, 10 µM R-α-methylhistamine (RAMH); H_4R, 1 µM JNJ-7777120). Specific binding was calculated by subtracting the nonspecific binding from total binding.

2.3. Determination of the intracellular concentration of Ca^{2+} ions ($[Ca^{2+}]_i$)

Cells grown in Petri dishes were detached by incubation with trypsin/EDTA solution, resuspended in 5 ml supplemented DMEM/F12 medium, and 300 µl aliquots were re-seeded on microfluorometry chambers previously coated with poly-L-Lysine (1 mg/10 ml). After incubation overnight at 37 °C in a CO_2 incubator, cells were rinsed twice with sterile PBS, and then incubated in DMEM/F12 medium containing probenecid (1 mM) and the fluorescent Ca^{2+} indicator dye Fura-2AM (2 µM). After 1 h at 37 °C, cells were washed with a modified Krebs-Ringer-HEPES (KRH) solution (in mM: NaCl 126, HEPES 10, D-glucose 11, KCl 3, $CaCl_2$ 2, $MgCl_2$ 1, pH 7.4 with NaOH), before incubation in this solution for 15 min at room temperature to allow for Fura-2AM de-esterification.

The chambers were placed on a TMD inverted microscope (Nikon, Japan) coupled to an RF-F3010 microfluorometer (Photon Technology International, South Brunswick, NJ), and cells were perfused (1 ml/min) with KRH solution. Drugs were applied by perfusion and changes in the $[Ca^{2+}]_i$ were determined by measuring the fluorescence ratio (510 nm) after excitation with lights of 340 and 380 nm wavelengths. Recordings were acquired at 20 Hz and the background fluorescence was determined in cell-free areas.

2.4. Determination of cAMP accumulation

Cells grown in 24-well plates were washed with KRH solution before incubation (37 °C) in 250 µl of the same solution containing 3-isobutyl-1-methylxanthine (IBMX, 1 mM). After 15 min, forskolin was added in a 10 µl volume (3 µM as final concentration) and incubations continued for 30 min. Agonist stock solutions (10 mM in dimethyl sulfoxide, DMSO) were dissolved in deionized water and added in a 10 µl volume 5 min before forskolin. Incubations were terminated by aspirating the medium and adding 250 µl ice-cold 0.1 M HCl. Plates were placed on ice for 15 min, and the contents were neutralized with 25 µl 1 M NaOH and 100 µl 1 M Tris-HCl (pH 7.0) before centrifugation (2,500 × *g*, 5 min at 4 °C). The composition of the KRH solution was (mM): NaCl 113, HEPES 20, $NaHCO_3$ 25, D-glucose 15, KCl 4.7, $CaCl_2$ 1.8, $MgCl_2$ 1.2, KH_2PO_4 1.2, pH 7.3 with NaOH.

The accumulation of cAMP was determined by competition between endogenous cAMP and [^{3}H]-cAMP for the regulatory subunit of protein kinase A (PKA) present in a crude supernatant from bovine adrenal

Table 1
Primary antibodies employed in this study.

Antibody		Source (Catalog number)	RRID	Dilution	Experiment
α-tubulin mouse monoclonal		Sigma-Aldrich (T9026)	AB_477753	1: 10,000	Western blot
α-CD11b/c (OX-42) mouse monoclonal	Microglia marker	Abcam (ab1211)	AB_442947	1: 200	Immunocytochemistry
α-ERK-1/2 rabbit monoclonal	Extracellular signal-regulated kinases	Cell Signaling (4695)	AB_390779	1: 1,000	Western blot
α-phospho-ERK-1/2 (Thr^{202}/Tyr^{204}) rabbit polyclonal	Phosphorylated ERK-1/2	Cell Signaling (9101)	AB_2315036	1: 1,000	Western blot
α-GFAP rabbit polyclonal	Astrocyte marker	Scientific Thermo Fisher (PA5-16291)	AB_10980769	1: 1,000	Immunocytochemistry
α-GLUT-1 rabbit polyclonal	Glucose Transporter 1	Millipore (07–1401)	AB_11212210	1: 3,000 1: 300	Western blot Immunocytochemistry
α-O4 mouse monoclonal	Oligodendrocyte marker	Millipore (MAB345)	AB_94872	1: 100	Immunocytochemistry

RRID, Resource Identification Portal. https://scicrunch.org/resources.

medulla. Samples (50 μl) were mixed with 75 μl of incubation buffer containing the crude supernatant and [^{3}H]-cAMP (10 nM). After incubation for 2.5 h at 4 °C, samples were filtered through glass-fiber paper, presoaked in 0.3% of polyethylenimine for 2 h, and filters were washed 3 times with ice-cold deionized water, transferred to plastic vials and 3 ml scintillator solution were added. The retained radioactivity was determined by liquid scintillation and cAMP accumulation was calculated by extrapolation to a standard cAMP curve (10^{-12} -10^{-5} M). The composition of the incubation buffer was: 50 mM Tris-HCl, 100 mM NaCl, 5 mM EDTA, 5 mg/ml bovine serum albumin (BSA), pH 7.0 at 4 °C.

2.5. Quantitative real-time PCR

Cells, grown in 6-well plates, were incubated with drugs under test in serum-free medium as described for Western blot analysis (Section 2.6.1), washed with ice-cold PBS and then scrapped in 500 μl TRIzol® (Thermo Scientific). Lysates were transferred to 1.5 ml Eppendorf tubes, chloroform (100 μl) was added, the tubes were vigorously shaken, left to stand for 3 min at room temperature, and centrifuged (13,000 × g, 15 min at 4 °C). The aqueous phase was collected and placed into sterile tubes to precipitate the RNA with 100% isopropanol (250 μl) by incubating for 30 min at room temperature and centrifuging (13,000 × g, 10 min at 4 °C). The supernatant was removed, and the pellet was washed twice with 1 ml 75% ethanol in water and centrifuged (7,500 × g, 5 min at 4 °C). After elimination of ethanol residues by evaporation, the pellet (RNA) was suspended in nuclease-free water (diethyl dicarbonate-treated).

Total RNA was quantified by measuring the optical density at 260/280 nm, and cDNA was synthesized using RNA (5 μg), random hexamers (50 ng/μl), deoxynucleotide trisphosphates (5 mM), M-MLV-RT reverse transcriptase (200 U/μl), RNAsin (20 U/μl), and M-MLV RT buffer to yield 25 μl as final volume. The reaction was incubated at 37 °C (1 h) and the expression of GLUT-1 mRNA transcripts was determined by quantitative RT-PCR using TaqMan® Universal PCR Master Mix (Applied Biosystems, Foster, CA), TaqMan® probe Rn01417099_m1 to detect GLUT-1, and TaqMan® probe Rn01455646_m1 to detect the TATA binding protein to normalize GLUT-1 expression. The PCR conditions were as follows: holding step, required for DNA polymerase activation, 50 °C (2 min) and 95 °C (10 min), followed by 45 cycles at 95 °C (15 s) for denaturalization and 60 °C (1 min) for extension/alignment. Samples were analyzed in triplicates and a no-template control was included. The relative expression of GLUT-1 was quantified by the $2^{-\Delta\Delta CT}$ method (Livak et al., 2001). PCR efficiency for both genes was > 95%.

2.6. Western blotting

2.6.1. GLUT-1

Cells were grown in Petri dishes (60 mm diameter), and upon confluence incubated overnight in serum-free medium. The day of the experiment the medium was exchanged for 3 ml serum-free medium and cells were incubated for 15 min in the incubator before the addition of drugs under test in a 60 μl volume and further incubation for the indicated times. Where required, antagonists were added 10 min before agonists. Drugs were dissolved in serum-free medium.

Incubations were terminated by aspirating the medium, and cells were washed with ice-cold PBS before adding RIPA solution (150 mM NaCl, 1% Igepal, 0.5% sodium deoxycholate, 50 mM Tris-HCl, pH 8.0) containing a protease inhibitor cocktail (P8340, Sigma-Aldrich, St Louis, MO). Cells were scrapped and homogenized by sonication for 5 s before centrifugation (13,000 × g, 13 min at 4 °C). Protein content in the supernatant was measured (BCA method), and samples (~10 μg protein) were separated on a 10% SDS-polyacrylamide gel, and then electroblotted onto polyvinylidene fluoride (PVDF) membranes (Bio Rad, Life Science Research, Hercules, CA). Membranes were blocked for 1 h at room temperature in TBS-T solution (20 mM Tris-HCl, pH 7.4, 0.05% Tween 20, and 150 mM NaCl) containing 5% milk powder (w/v). Membranes were then incubated overnight at 4 °C with primary antibodies anti-GLUT-1 (1:3,000; Millipore, Burlington, MA; Table 1) and anti-α-tubulin (1:10,000; Sigma-Aldrich) diluted in TBS-T with 3% BSA, washed with TBS-T and then incubated with the secondary antibody (anti IgG conjugated with horseradish peroxidase; 1:5,000) at room temperature for 1 h. Chemiluminescence was determined with C-DiGit Blot Scanner LI-COR (LI-COR Biosciences, Lincoln, NE), and the densitometric analysis was performed using ImageJ program (imagej.nih.gov).

2.6.2. Phosphorylated extracellular signal-regulated kinases ERK-1/2 (p44/p42-ERK)

The experimental protocol was similar to that described for GLUT-1 immunodetection. Primary antibodies were anti phospho-ERK-1/2 or anti ERK-1/2 (1:1,000; Cell Signaling, Danvers, MA; Table 1). The secondary antibody (1:5,000) was conjugated with horseradish peroxidase. Target bands were expressed quantitatively by normalization to the intensity of the non-phosphorylated ERK-1/2 signal on the same blot.

2.7. Confocal microscopy

Cells were seeded on glass coverslips (16 mm diameter), which were placed in 24-well plates before the addition of supplemented DMEM/F12 medium. Once confluence was reached, cells were incubated overnight in serum-free medium. Cells were then rinsed twice with sterile PBS, serum-free medium was added (500 μl per well) and cells were incubated for 15 min in the incubator before the addition of agonists in a 10 μl volume and further incubation for 3 h. Where required, antagonists were added 10 min before the agonists.

The medium was aspirated and cells were rinsed with ice-cold PBS before being fixed with 4% paraformaldehyde (10 min at room

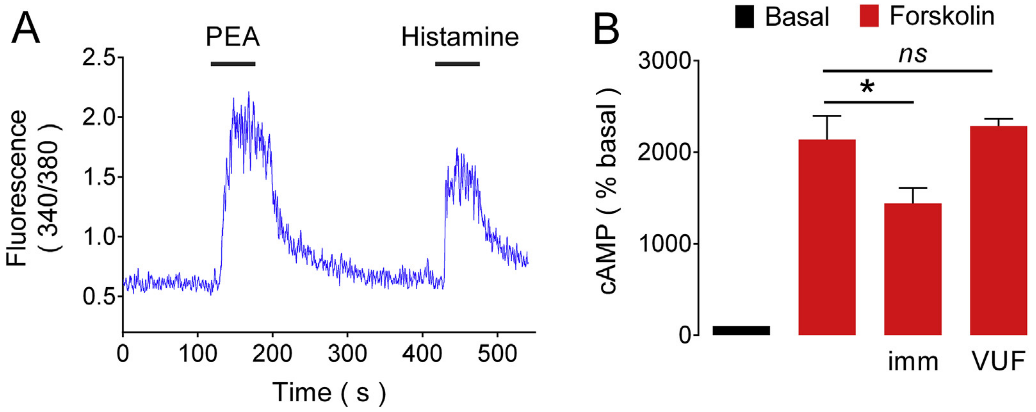

Fig. 1. Functional characterization of H_1Rs and H_3Rs expressed by rat cerebro-cortical astrocytes in primary culture. A. Cells were loaded with Fura-2AM as described in Materials and methods before being examined by microfluorometry under perfusion with the H_1R agonist 2-pyridyl-ethylamine (PEA, 30 μM) or histamine (30 μM) for 60 s, as indicated by the bars. A representative experiment, repeated a further 7 times, is illustrated. **B.** Cells grown in 24-well plates were incubated in Krebs-Ringer-HEPES solution containing IBMX (1 mM) before exposure to forskolin (10 μM) and the H_3R agonist immepip (imm, 100 nM) or the H_4R agonist VUF-8430 (VUF, 1 μM). Values are means ± SEM from 7 experiments; *ns*, no statistical difference, $^{*}P < 0.05$, one-way ANOVA and Tukey's test.

temperature). The excess of paraformaldehyde was removed and cells were washed 3 times with PBS containing 0.1% BSA under shaking. Cells were then blocked and permeabilized for 1 h at room temperature with PBS/1% BSA and 0.1% Triton X-100 and incubated with the anti-GLUT-1 primary antibody (1:300; Millipore; Table 1) for 2 h at room temperature. Cells were rinsed 3 times with PBS/0.1% BSA and then incubated with the secondary antibody conjugated with the fluorophore Alexa-647 (1:200; Thermo Scientific) at room temperature in the dark. After 1 h, cells were washed with PBS/1% BSA and incubated with Hoechst (10 mg/ml) for 10 min at room temperature in the dark. Finally, cells were rinsed 3 times with PBS and mounted with Vectashield mounting solution (Invitrogen, Carlsbad, CA) and visualized on a confocal microscope (DM6000 CS, Leica Microsystems, Wetzlar, Germany).

2.8. Data analysis

Data are presented as a means ± standard error (SEM). The statistical analysis was performed with one-way ANOVA followed by Dunnett's or Tukey's test.

2.9. Drugs

The following drugs were purchased from Sigma Aldrich: adenosine 3′,5′-cyclic monophosphate (cAMP), clobenpropit dihydrobromide, histamine dihydrochloride, immepip dihydrobromide, 3-isobutyl-1-methylxanthine (IBMX), mepyramine maleate, Ro-31-8220 (2-{1-[3-(Amidinothio)propyl]-1H-indol-3-yl}-3-(1-methylindol-3-yl)maleimide methanesulfonate salt), (R) (−)-α-methylhistamine dihydrochloride and UO126 monoethanolate. Amthamine dihydrobromide and dimaprit dihydrochloride were from Tocris (Minneapolis, MN). 2-Pyridyl-ethylamine (PEA) was a kind gift from Dr. John Michael Young (Department of Pharmacology, University of Cambridge). N-α-[methyl-^{3}H]-histamine (84.1 Ci/mmol), [^{3}H]-mepyramine (20 Ci/mmol), [^{3}H]-histamine (20 Ci/mmol) and [^{3}H]-cAMP ([2,8-^{3}H]-adenosine 3′,5′-cyclic phosphate; 25.4 Ci/mmol) were from PerkinElmer (Boston, MA). The primary antibodies employed are listed in Table 1.

3. Results

3.1. Rat cerebro-cortical astrocytes in primary culture express H_1Rs and H_3Rs

Astrocytes from rat cerebral cortex in primary culture express H_1Rs and H_3Rs in their cell membranes (Lipnik-Štangelj et al., 2004; Mele and Jurič, 2013). In this work, the presence of H_1Rs and H_3Rs in membranes from primary cerebro-cortical astrocytes was evaluated by assaying the binding of the selective H_1R antagonist [^{3}H]-mepyramine and the selective H_3R agonist [^{3}H]-NMHA.

The concentration of [^{3}H]-mepyramine assayed (10 nM) was near that required for saturating binding to H_1Rs expressed by human astrocytoma U373 MG cells (Arias-Montaño et al., 1994), and yielded a density of 230 ± 22 fmol/mg protein (5 determinations; Supplementary Figure 3), similar to values reported previously, 262 ± 60 fmol/mg protein (Inagaki et al., 1989) and 281 ± 53 fmol/mg protein (Lipnik-Štangelj and Carman-Krzan, 2004).

The density of [^{3}H]-NMHA binding sites (H_3Rs) was 11.9 ± 0.4 fmol/mg protein (4 determinations; Supplementary Figure 3). The concentration of [^{3}H]-NMHA assayed (4 nM) was close to the dissociation constant (*K*d) reported for cortical astrocytes in primary culture (4.55 nM; Mele and Juric, 2013). The *K*d equals the concentration required for occupancy of 50% of the total number of receptors, and the maximum density of H_3Rs should therefore approximate 24 fmol/mg protein, 4 fold the value (~6 fmol/mg protein) reported by Mele and Juric (2013).

3.2. Functional characterization of H_1Rs and H_3Rs

Through the activation of $G\alpha_{q/11}$ proteins, H_1Rs stimulate the activity of phospholipase C (PLC) leading to the mobilization of Ca^{2+} ions from intracellular stores and PKC activation (Panula et al., 2015). Accordingly, Fig. 1A shows that in rat cerebro-cortical astrocytes in primary culture both histamine and the selective H_1R agonist 2-pyridyl-ethylamine (PEA) increased the intracellular concentration of Ca^{2+} ($[Ca^{2+}]_i$). The response to PEA was observed in 15 of 31 cells that also responded to histamine with an increase in $[Ca^{2+}]_i$.

H_3Rs couple to $G\alpha_{i/o}$ proteins, whose activation triggers or modulates several signaling pathways, most notably the inhibition of adenylyl cyclase activity (Nieto-Alamilla et al., 2016), and Fig. 1B shows that in cultured astrocytes the H_3R agonist immepip significantly reduced forskolin-induced cAMP accumulation to 61.2 ± 6.5% of control values.

As mentioned before, astrocytes in culture express H_2Rs (Jurič et al., 2011, 2016), and their activation stimulates glycogenolysis (Arbones et al., 1990) and neurothrophin 3 synthesis via the cAMP/PKA pathway (Jurič et al., 2011). In this study, the selective H_2R agonists amthamine and dimaprit (30 μM) stimulated modestly, but significantly, cAMP accumulation in primary cerebro-cortical astrocytes (146.9 ± 2.1 and 152.3 ± 14.5% of basal values, respectively; Supplementary Figure 4), but failed to stimulate ERK-1/2 phosphorylation or GLUT-1 expression (see below).

Microglia cells have been shown to express functional H_4Rs (Ferreira et al., 2012; Dong et al., 2014), and a low number of cells immunoreactive to the microglia marker CD11b/c (OX42) was present

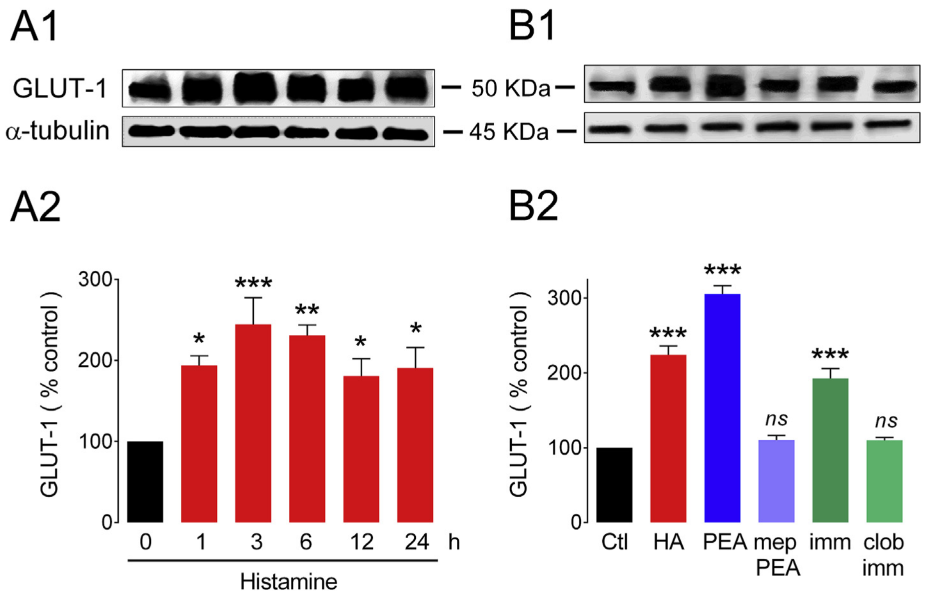

Fig. 2. Histamine increases GLUT-1 protein expression via H_1R and H_3R activation in cerebro-cortical astrocytes in primary culture. **A**. Time course of the histamine effect. Cells were incubated overnight in serum-free DMEM/F12 mixture and then with histamine (30 μM) for the indicated times. GLUT-1 protein was evaluated by Western blot. **A1.** Representative blot. **A2**. Analysis of 6 experiments. Values are means ± SEM. $^{*}P < 0.05$, $^{**}P < 0.01$, $^{***}P < 0.001$, with respect to control values; one-way ANOVA and Dunnett's test. **B**. Effect of selective H_1R and H_3R agonists and antagonists. Cells were incubated overnight in serum-free DMEM/F12 mixture and then for 3 h with histamine (HA, 30 μM), the H_1R agonist 2-pyridylethylamine (PEA, 30 μM) or the H_3R agonist immepip (imm, 100 nM). Where required, the H_1R antagonist mepyramine (mep, 1 μM) or the H_3R antagonist clobenpropit (clob, 1 μM) were added 10 min before the corresponding agonist. **B1**. Representative blot. **B2**. Analysis of 8 experiments. Values are means ± SEM. *ns*, no significant difference; $^{***}P < 0.001$ versus control values (Ctl), one-way ANOVA and Tukey's test.

in the astrocyte-enriched cultures (Supplementary Figure 2). However, the selective H_4R antagonist JNJ-7777120 did not inhibit [^{3}H]-histamine binding in membranes from the same cultures (Supplementary Figure 3C). Furthermore, H_4Rs couple to $G\alpha_{i/o}$ proteins, but receptor activation with the agonist VUF-8430 failed to inhibit cAMP accumulation (Fig. 1B).

Altogether, these results show the presence of functional H_1Rs and H_3Rs in the primary cultures of rat cerebro-cortical astrocytes employed in this study, confirm the absence of H_4R expression, and indicate low H_2R expression.

3.3. *H_1R- and H_3R-activation increases GLUT-1 protein*

In the brain parenchyma, GLUT-1 is mainly located on astrocytes (Maher et al., 1994; McCall et al., 1996; Yu and Ding, 1998). To evaluate the effect of histamine on the expression of GLUT-1 protein by rat cerebro-cortical astrocytes, primary cultures were exposed to histamine for 1–24 h. Fig. 2 (panels A1 and A2) shows that histamine significantly increased GLUT-1 protein at all times tested, with a peak at 3 h (244 ± 34% of control values). The effect of histamine was mimicked by selective agonists at H_1Rs (PEA) and H_3Rs (immepip), and the H_1R antagonist mepyramine prevented the PEA effect, while the H_3R antagonist clobenpropit blocked the action of immepip (Fig. 2, panels B1 and B2), indicating the participation of both H_1Rs and H_3Rs. In a different series of experiments, the selective H_2R agonist dimaprit (30 μM) increased GLUT-1 protein levels to 122.6 ± 8.8% of control values (7 experiments), but the effect did not yield statistical significance (Supplementary Figure 5). A lack of effect was also observed for the H_4R agonist VUF-8430 (1 μM, 108.6 ± 5.3% of control values). The stimulatory effect of the H_1R agonist PEA and the H_3R agonist immepip was confirmed in these experiments.

To test for additive effects of H_1R and H_3R activation, primary cerebro-cortical astrocytes were incubated with the H_1R agonist PEA or the H_3R agonist immepip, and the combination of both agonists. Supplementary Figure 6 shows a lack of additivity of PEA and immepip (PEA, 167.3 ± 10.3% of control values; immepip, 164.9 ± 4.9%; PEA + immepip, 156.9 ± 5.0%; histamine, 179.6 ± 8.1%).

The increase in GLUT-1 protein expression induced by histamine and H_1R or H_3R activation was confirmed by immunocytochemistry and confocal microscopy (Fig. 3). Altogether, these results support that the effect of histamine on GLUT-1 protein expression is primarily mediated by H_1R and H_3R activation.

3.4. *H_1R and H_3R activation increases GLUT-1 mRNA expression*

Fig. 4A shows that histamine (30 μM) increased GLUT-1 mRNA expression by rat cerebro-cortical astrocytes at 1, 2 and 3 h incubations, with no significant differences. Exposure for 1 h to histamine, the H_1R agonist PEA or the H_3R agonist immepip increased GLUT-1 mRNA expression by rat cerebro-cortical astrocytes to a similar extent (153.4 ± 6.5%, 163 ± 2.2% and 168 ± 13.2% of control values, respectively), and the selectivity of the agonist effect was confirmed by the blockade by the corresponding antagonist (Fig. 4B).

3.5. *Effect of PKC inhibition on H_1R- and H_3R-induced GLUT-1 protein expression*

PKC activates the MAPK pathway by directly phosphorylating Raf-1 or via a Ras-dependent pathway (Rozengurt, 2007; Roskoski et al., 2012), and Fig. 5 (panels A1 and A2) shows that the general PKC inhibitor Ro-318220 prevented the effect of histamine and H_1R and H_3R agonists. These results indicate that PKC participates in the H_1R- and H_3R-mediated increase in GLUT-1 expression in primary astrocytes.

Typically, PKC activation results from the stimulation by $G\alpha_{q/11}$ proteins of PLC activity (Steinberg, 2008; Zeng et al., 2012), leading to the formation of diacylglycerol (DAG) and inositol 1,4,5-trisphosphate (IP_3). IP_3 induces Ca^{2+} mobilization upon binding to receptors located on intracellular Ca^{2+} stores, and in transfected cells H_3R activation increases the $[Ca^{2+}]i$ (Cogé et al., 2001; Bongers, 2008). To evaluate the coupling of H_3Rs to PLC activation, cultured cortical astrocytes were exposed to the H_3R agonists immepip and RAMH, which increased the $[Ca^{2+}]i$ in cells that also responded to histamine or the H_1R agonist PEA (Supplementary Figure 7).

3.6. *Effect of MEK-1/2 inhibition on H_1R- and H_3R-induced GLUT-1 protein expression*

In 3T3-L1 adipocytes, endothelin-1 increased GLUT-1 mRNA and glucose uptake, and the latter effect was reduced by inhibiting the MAPK pathway (Fong et al., 2001). In rat cerebro-cortical astrocytes histamine induced ERK-1/2 phosphorylation, which was statistically different from control values at 1 and 5 min incubations (125.6 ± 6.2 and 146.8 ± 8.9%, respectively), returning afterwards to levels not significantly different from control values. The effect of histamine was mimicked by the H_1R agonist PEA and the H_3R agonist immepip, but

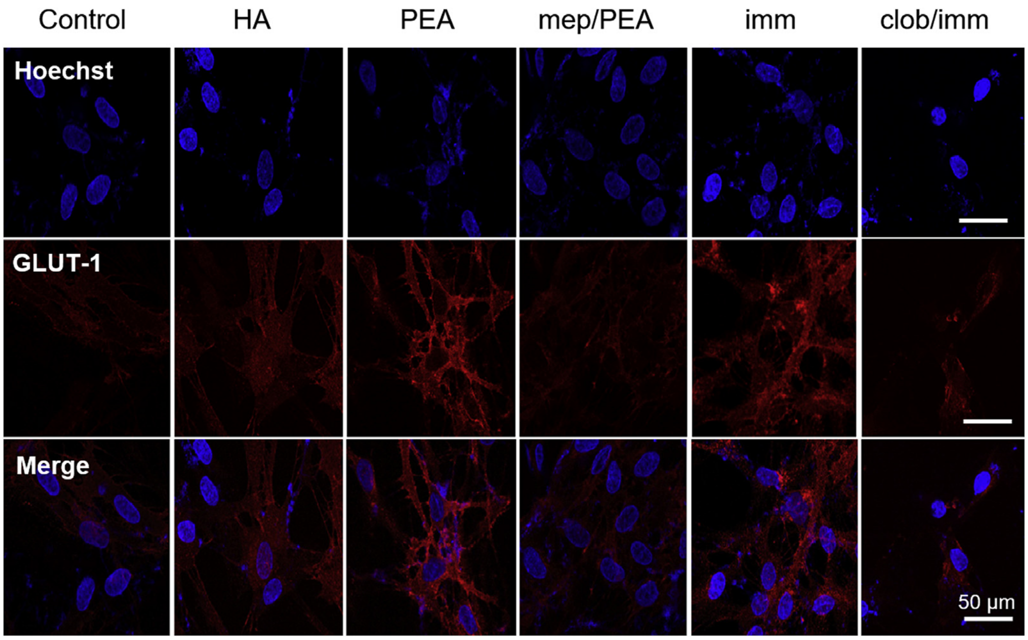

Fig. 3. H_1R and H_3R activation increases GLUT-1 protein expression by cerebro-cortical astrocytes in primary culture as evaluated by immunocytochemistry. Cells were incubated overnight in serum-free DMEM/F12 mixture and then for 3 h with histamine (HA, 30 µM), the H_1R agonist 2-pyridyl-ethylamine (PEA, 30 µM) or the H_3R agonist immepip (imm, 100 nM). Where required, the H_1R antagonist mepyramine (mep, 1 µM) or the H_3R antagonist clobenpropit (clob, 1 µM) were added 10 min before the corresponding agonist. Confocal microscopy images are representative of 3 experiments with different cultures.

not by H_2R or H_4R agonists (Supplementary Figure 8).

Fig. 5 (panels B1 and B2) shows that in cortical astrocytes MEK-1/2 inhibition by UO126 reduced by 70% the effect of histamine on GLUT-1 protein expression, making it not statistically different from control values, and reduced by 56% the effect of H_1R activation, although in this case the remaining effect was statistically different from both control and histamine-stimulated GLUT-1 expression. Furthermore, MEK-1/2 inhibition fully prevented the effect of H_3R activation. The MEK-1/2 inhibitor UO126 had no effect on its own on GLUT-1 protein expression (103.2 ± 3.2% of control values, 4 determinations, not illustrated). These results indicate that the MAPK pathway participates in the effect of histamine on GLUT-1 expression, mediating in full the effect of H_3R activation and partially the effect of H_1R activation.

4. Discussion

A significant fraction (~40%) of the glucose captured by astrocytes is destined to glycogen synthesis (Prebil et al., 2011; Hutchinson et al., 2011), allowing for the production of lactate via glycolysis or glycogenolysis in response to neuronal activity (Duelli and Kuschinsky, 2001; Simpson et al., 2007; Nehlig and Coles, 2007; Pellerin et al., 2007). Astrocytes express the 45 kDa form of GLUT-1, and in this work we show that rat cerebro-cortical astrocytes in primary culture express functional H_1Rs and H_3Rs, whose stimulation increases GLUT-1 expression, involving PKC and MAPK activation.

4.1. Histamine-induced GLUT-1 expression by primary rat cerebro-cortical astrocytes is mediated by both H_1R and H_3R activation

Previous work reported that primary rat cortical astrocytes express mRNA for H_1Rs, H_2Rs and H_3Rs, but not for H_4Rs, with H_3R mRNA levels being 7- to 8-fold lower than for H_2R or H_1R mRNA (Jurič et al., 2011). Similar results were obtained by mRNA and Western blot analysis in cultured astrocytes obtained from the rat whole brain (Xu et al., 2018). In this work, binding assays confirmed the presence of H_1Rs and H_3Rs and the absence of H_4Rs. The functionality of the detected H_1Rs, coupled to $G\alpha_{q/11}$ proteins and thus to PLC activation, was evidenced by the increase in the $[Ca^{2+}]i$ induced by histamine and the selective agonist PEA. H_3Rs couple to $G\alpha_{i/o}$ proteins, and the inhibition of forskolin-induced cAMP accumulation by the selective agonist immepip confirmed the functionality of H_3Rs expressed by primary astrocytes.

Our data show that in cerebro-cortical astrocytes histamine increased both GLUT-1 mRNA and protein levels and that this effect was mimicked by selective agonists at H_1Rs and H_3Rs. Moreover, the effects of the agonists were prevented by selective antagonists, mepyramine and clobenpropit, respectively, indicating that histamine-induced GLUT-1 expression is mediated by the activation of either H_1Rs or H_3Rs.

Astrocytes in culture express H_2Rs (Jurič et al., 2011, 2016), and the

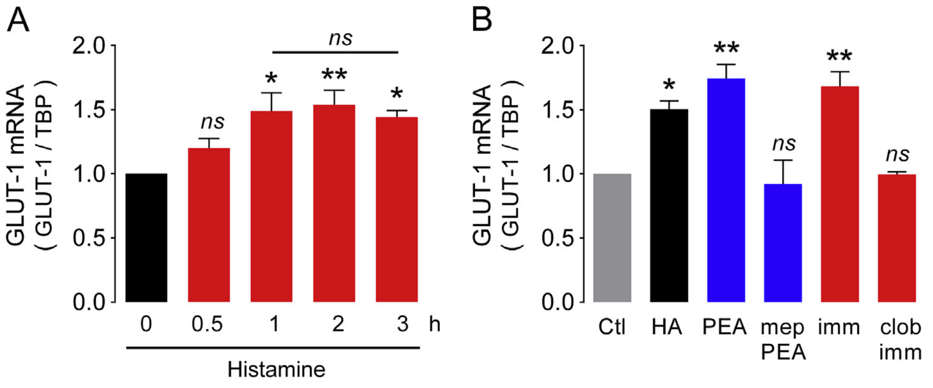

Fig. 4. H_1R and H_3R activation increases GLUT-1 mRNA expression by cerebro-cortical astrocytes in primary culture. A. Time course for the effect of histamine. Cells, grown in 6-well plates, were incubated overnight in serum-free DMEM/F12 mixture and then in the absence or presence of histamine (30 µM) for the indicated times. Values are means ± SEM from 3 experiments. *ns,* no significant difference versus control values (without histamine) or among 1, 2 and 3 h incubations; $^{*}P < 0.05$, $^{**}P < 0.01$ versus control values; one-way ANOVA and Tukey's test. **B**. Effect of selective H_1R and H_3R agonists and antagonists. Cells were incubated for 1 h with histamine (HA, 30 µM), the H_1R agonist 2-pyridyl-ethylamine (PEA, 30 µM) or the H_3R agonist immepip (imm, 100 nM). Where required, the H_1R antagonist mepyramine (mep, 1 µM) or the H_3R antagonist clobenpropit (clob, 1 µM) were added 10 min before the corresponding agonist. Values are means ± SEM from 3 experiments. *ns,* no significant difference, $^{*}P < 0.05$, $^{**}P < 0.01$ versus control values (Ctl); one-way ANOVA and Dunnett's test.

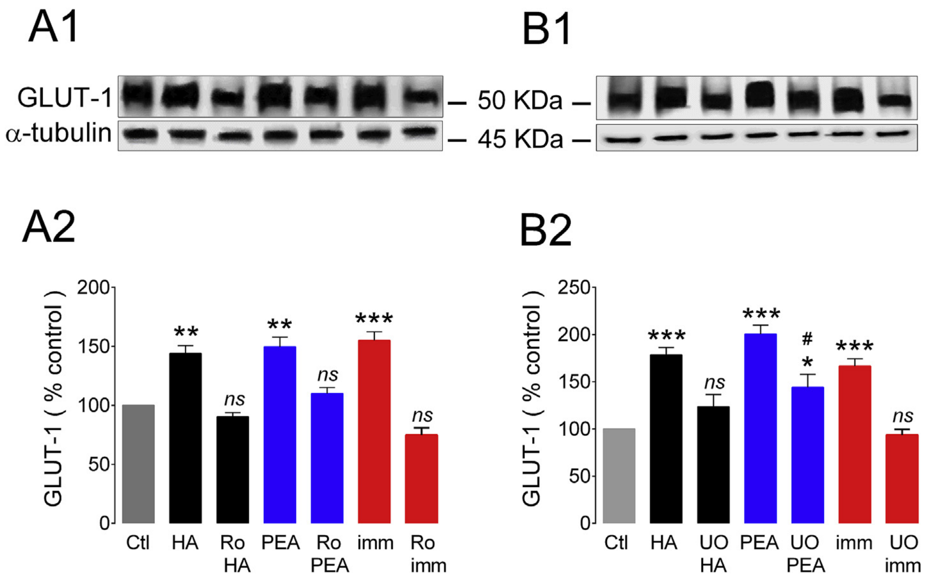

Fig. 5. Effect of PKC or MEK-1/2 inhibition on H_1R- and H_3R-induced GLUT-1 protein expression. A. PKC inhibition. Cells were incubated overnight in serum-free DMEM/F12 mixture before exposure for 3 h to histamine (HA, 30 μM), the H_1R agonist 2–ethylamine (PEA, 30 μM) or the H_3R agonist immepip (imm, 100 nM). Where required, the general PKC inhibitor Ro-318220 (Ro, 200 nM) was added 30 min before the agonists. **A1**. Representative blot. **A2**. Analysis of 5 experiments; values are means ± SEM. *ns,* no significant difference; $^{**}P < 0.01$, $^{***}P < 0.001$, with respect to control values (Ctl); one-way ANOVA and Dunnett's test. **B.** Effect of MEK-1/2 inhibition. Cells were incubated overnight in serum-free DMEM/F12 mixture and then for 3 h with histamine (HA, 30 μM), the H_1R agonist 2-pyridyl-ethylamine (PEA, 30 μM) or the H_1R agonist immepip (imm, 100 nM). Where required, the MEK-1/2 inhibitor UO126 (UO, 10 μM) was added 15 min before the agonists. **B1**. Representative blot. **B2**. Analysis of 6 experiments. Values are means ± SEM. *ns*, no significant difference; $^{***}P < 0.00$ with respect to control values (Ctl); $^{\#}P < 0.05$ compared with PEA alone; one-way ANOVA and Tukey's test.

H_2R agonist dimaprit (10 nM-1 μM) stimulates neurothrophin 3 synthesis via the cAMP/PKA pathway (Jurič et al., 2011), and increases glycogenolysis (Arbones et al., 1990), although at a very high concentration (1 mM). In our experiments H_2R activation increased modestly cAMP accumulation, but failed to stimulate GLUT-1 expression or ERK-1/2 phosphorylation (Supplementary Figures 4, 5 and 8). The discrepancies with previous studies may rely on the different functional responses measured, as well as on the low H_2R expression in our cultures suggested by the modest effect on cAMP accumulation. In turn, culture conditions may account for variations in receptor expression, although the only difference with the studies of Jurič et al. (2011) and Arbonés et al. (1990) appears to be the addition of hydrocortisone and sodium selenite to the medium employed in this study.

4.2. *Mechanisms likely to underlie the effect of H_1R and H_3R activation on GLUT-1 protein expression by cerebro-cortical astrocytes*

In 3T3-L1 adipocytes endothelin-1 stimulates GLUT-1 transcription via ET_A receptors, activation of $G\alpha_{i/o}$ proteins and PKC- and MAPK-dependent pathways (Fong et al., 2001; Kao and Fong, 2008a,b). For primary cerebro-cortical astrocytes, we found that the general PKC inhibitor Ro-31822 prevented H_1R- and H_3R-induced GLUT-1 protein expression, indicating that the signaling mechanism triggered by both receptors converge at PKC activation (see Fig. 5). In bovine mammary epithelial cells, PKC activation by phorbol 12-O-tetradecanoate-13-acetate (TPA) increases GLUT-1 mRNA levels and this effect was prevented by the PKC inhibitor GF1090203X (Zhao et al., 2014), whereas in 3T3-L1 adipocytes exposure to prostaglandin F2α increased GLUT-1 protein and mRNA levels, and these effects were prevented by depletion of DAG-sensitive PKCs by prolonged treatment with TPA (Chiou and Fong, 2004). Furthermore, in mesangial cells PKC inhibition prevented the up-regulation of GLUT-1 mRNA levels induced by angiotensin II (Nose et al., 2003). Altogether, this information supports that PKC activation regulates GLUT-1 expression.

PKC isoenzymes are classified into 3 classes on the basis of their molecular structure and requirement for DAG and Ca^{2+} for their activation: classical (α, βI, βII and γ), which require DAG and Ca^{2+}; novel (δ, ε, η and θ), which require only DAG; and atypical (ξ and λ), activated by mechanisms that do not require DAG or Ca^{2+} (Steinberg, 2008; Zeng et al., 2012). H_1Rs couple to $G\alpha_{q/11}$ proteins and thus to PLC activity (Panula et al., 2015) leading to the formation of DAG and IP_3, and the latter induces Ca^{2+} mobilization upon binding to receptors located on intracellular Ca^{2+} stores. Therefore, H_1R activation can stimulate classical and novel PKCs. In this work, H_3R activation increased the $[Ca^{2+}]$i in a fraction of primary cortico-cerebral astrocytes (Supplementary Figure 7), and the H_3R-mediated increase in GLUT-1 protein levels was fully prevented by PKC inhibition (Fig. 5). These results indicate that H_3R activation also stimulates PLC activity leading to DAG production and PKC activation.

In transfected CHO and SK-N-MC cells activation of the human H_3R of 445 amino acids (hH_3R_{445}) increases the $[Ca^{2+}]$i (Cogé et al., 2001; Bongers, 2008), and in SK-N-MC cells the effect involves PLC activation and Ca^{2+} release from intracellular stores via IP_3 formation (Bongers, 2008). Furthermore, in a subpopulation of striatal neurons in primary culture H_3R activation stimulates PLC activity and Ca^{2+} mobilization (Rivera-Ramírez et al., 2016).

The fact that an increase in the $[Ca^{2+}]_i$ in response to H_3R activation was only observed in a fraction of cells that responded to H_1R activation, could be explained by lower PLC stimulation and IP_3 formation, compared with that produced by H_1R activation. Low intracellular IP_3 concentrations lead to sporadic, small localized elevations of the $[Ca^{2+}]_i$ (blips). As the IP_3 concentration increases, more IP_3 receptors are recruited and produce intermediate events ('Ca^{2+} puffs'). At even higher IP_3 concentrations, more puffs are ignited and their spatiotemporal summation leads to a global Ca^{2+} wave that spreads throughout the cell (Rahman, 2012), as those recorded in our experiments. Thus, only in a fraction of cultured astrocytes IP_3 formation induced by H_3R activation appears to reach the threshold of global Ca^{2+} responses. This condition can also explain why the increase in $[Ca^{2+}]$i induced by PEA was observed in a fraction (48%) of those cells that also responded to histamine, because PEA acts as partial agonist at H_1Rs (Martinez-Mir et al., 1992; Tabarean, 2013), resulting thus in reduced signaling efficacy.

In regard to the MAPK pathway, in primary cerebro-cortical astrocytes H_1R and H_3R agonists induced ERK-1/2 phosphorylation (Supplementary Figure 8), and the stimulatory effect on GLUT-1 expression induced by H_1R or H_3R activation was reduced (−56%) or prevented, respectively, by the MEK-1/2 inhibitor UO126 (Fig. 5), indicating that downstream PKC activation, the H_1R- and H_3R-mediated actions depend partially or fully on the MAPK pathway. This result is in accord with the full or marked inhibition by the MAPK signaling inhibitor PD98059 of the increase in GLUT-1 mRNA induced by endothelin-1 in 3T3-L1 adipocytes (Fong et al., 2001) or the PKC-dependent up-regulation of GLUT-1 expression induced by angiotensin II in

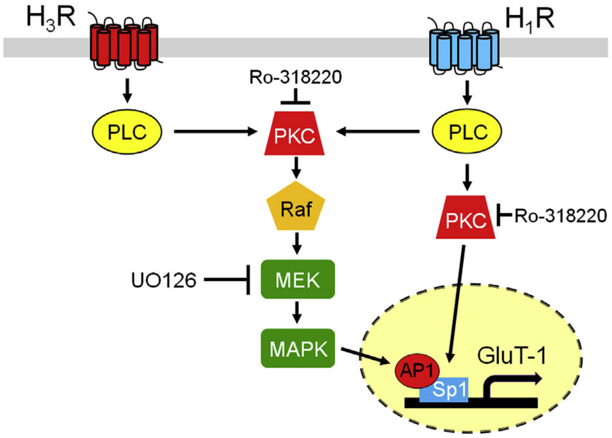

Fig. 6. Proposed mechanisms for the stimulatory effect of H_1 and H_3 receptor activation on GLUT-1 protein expression. The site of action of the inhibitors employed is indicated. H_1R, histamine H_1 receptor; H_3R, histamine H_3 receptor; MAPK, mitogen-activated protein kinase; PKC, protein kinase C; PLC, phospholipase C.

mesangial cells (Nose et al., 2003). Furthermore, in both HEK-293 cells transfected with the human H_3R and mouse primary cerebro-cortical neurons, H_3R-mediated ERK-1/2 phosphorylation depends on the activation of the PLC/PKC pathway by $G\beta\gamma$ subunits released from $G\alpha_{i/o}$ proteins (Lai et al., 2016).

The transcription factor Specificity Protein 1 (Sp1) is required for transcription of a large number of 'housekeeping' genes, but also regulates the expression of genes that contain putative CG-rich binding sites in their promoters (Vizcaino et al., 2015; Beishline and Azizkhan-Clifford, 2015). The GLUT-1 proximal promoter contains a consensus Sp1 binding site, which in rat cardiac cells plays a major role in GLUT-1 gene transcription and is essential for maintaining a high transcriptional activity (Santalucía et al., 2003; Hwang and Ismail-Beigi, 2001). Noteworthy, Sp1 can be phosphorylated by PCK and ERK-1/2 (Kao and Fong, 2008b, 2011; Beishline and Azizkhan-Clifford, 2015), and could therefore be involved in the H_1R- and H_3R-induced GLUT-1 up-regulation reported in this study.

Members of the AP-1 transcription factor family bind to consensus DNA-binding sites, known as TPA-response elements, TREs, and cyclic AMP-responsive elements, CREs (Kappelmann et al., 2014). In cardiac myocytes and via the MAPK pathway, hypertrophic stimuli induce the formation of cFos-containing AP-1 dimers, leading to GLUT-1 transcription (Santalucía et al., 2003). Therefore, GLUT-1 up-regulation induced by H_1R and H_3R activation reported in this study could also involve PKC- and MAPK-mediated AP-1 stimulation. Another possible mechanism for histamine-induced PKC-mediated increased GLUT-1 expression is the PKC-mediated phosphorylation of PPARγ1 and PPARγ2, shown to alleviate the repression of GLUT transcription exerted by the binding of the dimer PPARγ/retinoid X receptor-α to a GLUT promoter region (Suh and Han, 2013).

The effects of the H_1R and H_3R agonists were not additive (Supplementary Figure 6), suggesting the convergence of the signaling mechanisms triggered by these receptors, and the lack of effect of histamine and H_1R and H_3R agonists after PKC inhibition indicates that this kinase represents the point of convergence. Noteworthy, in spite of the significantly lower expression of H_3Rs, their activation increased GLUT-1 mRNA and protein levels to an extent similar to that induced by H_1R activation. One explanation is that DAG levels produced by H_3R-induced PLC stimulation suffice for PKC activation, and that in turn H_1R-induced DAG production exceeds the required levels. However, this hypothesis requires experimental testing.

Finally, TNF-α and endothelin-1 increase the half-life of GLUT-1 mRNA (Cornelius et al., 1990; Fong et al., 2004), and histamine increases the half-life of IL-1β mRNA from 1.2 to 2.4 h (Vannier and Dinarello, 1993; Srinivasan et al., 2004). Therefore, although our results show that H_1R and H_3R activation induces GLUT-1 transcription, we cannot discard that enhanced stability of GLUT-1 mRNA contributes to the increase in GLUT-1 protein levels.

5. Conclusion

Histamine, acting at both H_1 and H_3 receptors, increases GLUT-1 expression by rat cerebro-cortical astrocytes in primary culture. The effect of H_1R activation appears to involve the PLC → DAG/Ca^{2+} → PKC and PLC → DAG/Ca^{2+} → PKC → MAPK pathways, while the H_3R-mediated action seems to rely only on the PLC → DAG/Ca^{2+} → PKC → MAPK pathway (Fig. 6). Histamine-induced GLUT-1 up-regulation may allow astrocytes to supply neurons with the metabolic substrates required for synaptic transmission, particularly during high-activity states, in which the firing of the histaminergic neurons is also at its highest (Panula and Nuutinen, 2013).

Author contributions

J. P.-A., P. A. and J.-A. A.-M. designed the study; J. P.-A., N. R.-R., L.-F. V.-M., U. G.-H. and P. A. performed experiments, J. P.-A., N. R.-R., U. G.-H., P. A. and J.-A. A.-M. performed data analysis. J. P.-A., P. A. and J.-A. A.-M. wrote the manuscript. All authors revised and approved the manuscript.

Funding

This work was supported by Cinvestav (Proyecto SEP-Cinvestav 166 to J.-A. A.-M.), Instituto Nacional de Neurología y Neurocirugía and Conacyt (grants CB-2012-01-182266 to P. A. and 220448 to J.-A. A.-M.). The funding sources were not involved at all in the study design, collection, analysis and interpretation of data, writing of the manuscript or the decision to submit this report.

Declaration of competing interest

The authors disclose no conflict of interest.

Acknowledgements

J.P.-A., N.R.-R. and L.-F.V.-M. held Conacyt graduate scholarships (231171, 282310 and 854628). We are grateful to Dr. Pavel Montes-de-Oca Balderas and Dr. Gerardo Contreras-Patiño for valuable discussions. We thank Dr. Juan Escamilla-Sánchez and Raúl González-Pantoja for excellent technical support.

Appendix A. Supplementary data

Supplementary data related to this article can be found at https://doi.org/10.1016/j.neuint.2019.104565.

References

Araque, A., Carmignoto, G., Haydon, P.G., 2001. Dynamic signaling between astrocytes and neurons. Annu. Rev. Physiol. 63, 795–813. https://doi.org/10.1146/annurev.physiol.63.1.795.

Arbonés, L., Picatoste, F., García, A., 1990. Histamine stimulates glycogen breakdown and increase $^{45}Ca^{2+}$ permeability in rat astrocytes in primary culture. Mol. Pharmacol. 37, 921–927.

Arias-Montaño, J.A., Berger, V., Young, J.M., 1994. Calcium-dependence of histamine- and carbachol-induced inositol phosphate formation in human U373 MG astrocytoma cells: comparison with HeLa cells and brain slices. Br. J. Pharmacol. 111, 598–608. https://doi.org/10.1111/j.1476-5381.1994.tb14779.x.

Augustin, R., 2010. The protein family of glucose transport facilitators: it's not only about glucose after all. IUBMB Life 62, 315–333. https://doi.org/10.1002/iub.315.

Beishline, K., Azizkhan-Clifford, J., 2015. Sp1 and the 'hallmarks of cancer'. FEBS J. 282, 224–258. https://doi.org/10.1111/febs.13148.

Bongers, G.M., 2008. Signal Transduction of the Histamine H_3 Receptor. PhD Thesis. Vrije

Universiteit Amsterdam. http://dare.ubvu.vu.nl/bitstream/handle/1871/15988/8192.pdf?sequence=5.

Carruthers, A., DeZutter, J., Ganguly, A., Devaskar, U.S., 2009. Will the original glucose transporter isoform please stand up!. Am. J. Physiol. Endocrinol. Metab. 297, 836–849. https://doi.org/10.1152/ajpendo.00496.2009.

Chiou, G.Y., Fong, J.C., 2004. Prostaglandin F2α increases glucose transport in 3T3-L1 adipocytes through enhanced GLUT1 expression by a protein kinase C-dependent pathway. Cell. Signal. 16, 15–21. https://doi.org/10.1016/j.cellsig.2003.09.001.

Cogé, F., Guénin, S.P., Audinot, V., Renouard-Try, A., Beauverger, P., Macia, C., Ouvry, C., Nagel, N., Rique, H., Boutin, J.A., Galizzi, J.P., 2001. Genomic organization and characterization of splice variants of the human histamine H_3 receptor. Biochem. J. 355, 279–288. https://doi.org/10.1042/bj3550279.

Cornelius, P., Marlowe, M., Pekala, P.H., 1990. Regulation of glucose transport by tumor necrosis factor-alpha in cultured murine 3T3-L1 fibroblast. J. Trauma 12, S15–S20. https://doi.org/10.1097/00005373-199012001-00006.

Dong, H., Zhang, W., Zeng, X., Hu, G., Zhang, H., He, S., Zhang, S., 2014. Histamine induces upregulated expression of histamine receptors and increases release of inflammatory mediators from microglia. Mol. Neurobiol. 49, 1487–1500. https://doi.org/10.1007/s12035-014-8697-6.

Duelli, R., Kuschinsky, 2001. Brain glucose transporters: Relationship to local energy demand. News Physiol. Sci. 16, 71–76. https://doi.org/10.1152/physiologyonline.2001.16.2.71.

Fellin, T., Carmignoto, G., 2004. Neuron to astrocyte signaling in the brain represents a distinct multifunctional unit. J. Physiol. 559, 3–15. https://doi.org/10.1113/jphysiol.20040063214.

Ferreira, S., Santos, T., Gonçalves, J., Baltazar, G., Ferreira, L., Agasse, F., Bernardino, L., 2012. Histamine modulates microglia function. J. Neuroinflammation 9, 90. https://doi.org/10.1186/1742-2094-9-90.

Fong, J.C., Kao, Y.S., Tsai, H., Ho, L.T., 2001. Endothelin-1 increases glucose transporter GLUT-1 mRNA accumulation in 3T3-L1 adipocytes by a mitogen-activated protein kinase-dependent pathway. Cell. Signal. 13, 491–497. https://doi.org/10.1016/S0898-6568(01)00174-7.

Fong, J.C., Kao, Y.S., Tsai, H., Chiou, Y.Y., Chiou, G.Y., 2004. Synergistic effect of endothelin-1 and cyclic AMP on glucose transport in 3T3-L1 adipocytes. Cell. Signal. 16, 811–821. https://doi.org/10.1016/j.cellsig.2003.12.004.

Haas, H.L., Sergeeva, O.A., Selbach, O., 2008. Histamine in the nervous system. Physiol. Rev. 88, 1183–1241. https://doi.org/10.1152/physrev.00043.2007.

Hutchinson, D.S., Catus, S.L., Merlin, J., Summers, R.J., Gibbs, M.E., 2011. α_2-Adrenoreceptors activate noradrenaline-mediated glycogen turnover in chick astrocytes. J. Neurochem. 117, 915–926. https://doi.org/10.1111/j.1471-4159.2011.07261.x.

Hwang, D.Y., Ismail-Beigi, F., 2001. Stimulation of GLUT-1 glucose transporter expression in response to hyperosmolarity. Am. J. Physiol. Cell Physiol. 281, C1365–C1372. https://doi.org/10.1152/ajpcell.2001.281.4.C1365.

Inagaki, N., Fukui, H., Taguchi, Y., Wang, N.P., Yamatodani, A., Wada, H., 1989. Characterization of histamine H_1-receptors on astrocytes in primary culture: [^{3}H] mepyramine binding studies. Eur. J. Pharmacol. 173, 43–51. https://doi.org/10.1016/0014-2999(89)90007-1.

Jurič, D.M., Mele, T., Carman-Kržan, M., 2011. Involvement of histaminergic receptor mechanism in the stimulation of NT-3 synthesis in astrocytes. Neuropharmacology 60, 1309–1317. https://doi.org/10.1016/j.neuropharm.2011.01.019.

Jurič, D.M., Kržan, M., Lipnik-Štangelj, D.M., 2016. Histamine and astrocyte function. Pharmacol. Res. 111, 774–783. https://doi.org/10.1016/j.phrs.2016.07.035.

Kao, Y.S., Fong, J.C., 2008a. Endothelin-1 induction of GLUT-1 transcription in 3T'-L1-adipocytes involves distinct PKCε and p42/44 MAPK-dependent pathways. Bioquim Biophys Acta 1780, 154–159. https://doi.org/10.1016/j.bbagen.2007.11.013.

Kao, Y.S., Fong, J.C., 2008b. Endothelin-1 induces GLUT-1 transcription through enhanced interaction between Sp1 and NF-κB transcription factors. Cell. Signal. 20, 771–778. https://doi.org/10.1016/j.cellsig.2007.12.012.

Kao, Y.S., Fong, J.C., 2011. A novel cross-talk between endothelin-1 and cyclic AMP signaling pathways in the regulation of GLUT1 transcription in 3T3-L1 adipocytes. Cell. Signal. 23, 901–910. https://doi.org/10.1016/j.cellsig.2011.01.016.

Kappelmann, M., Bosserhoff, A., Kuphal, S., 2014. AP-1/c-Jun transcription factors: regulation and function in malignant melanoma. Eur. J. Cell Biol. 93, 76–81. https://doi.org/10.1016/j.ejcb.2013.10.003.

Lai, X., Ye, L., Liao, Y., Jin, L., Ma, Q., Lu, B., Sun, Y., Shi, Y., Zhou, N., 2016. Agonist-induced activation of histamine H_3 receptor signals to extracellular signal-regulated kinases 1 and 2 through PKC-, PLD-, and EGFR-dependent mechanisms. J. Neurochem. 137, 200–215. https://doi.org/10.1111/jnc.13559.

Lipnik-Štangelj, Čarman-Kržan, 2004. Activation of histamine H_1-receptor enhances neurotrophic factor secretion from cultured astrocytes. Inflamm. Res. 53, 245–252. https://doi.org/10.1007/s00011-004-1247-3.

Livak, J.K., Schmittgen, D.T., 2001. Analysis of relative gene expression data using real time quantitative PCR and the $2_T^{-\Delta\Delta C}$ method. Methods 25, 402–408. https://doi.org/10.1006/meth.2001.1262.

Maher, F., Vannucci, S.J., Simpson, I.A., 1994. Glucose transporter proteins in brain. J Fed Am Soc Exp Biol 8, 1003–1011. https://doi.org/10.1096/fasebj.8.13.7926364.

Martínez-Mir, M.I., Estañ, L., Morales-Olivas, F.J., Rubio, E., 1992. Effect of histamine analogues on human isolated myometrial strips. Br. J. Pharmacol. 107, 528–531. https://doi.org/10.1111/j.1476-5381.1992.tb12778.x.

McCall, A.L., Van Bueren, M., Nipper, V., Moholt-Siebert, M., Downes, H., Lessov, N., 1996. Forebrain ischemia increases GLUT1 protein in brain microvessels and parenchyma. J. Cereb. Blood Flow Metab. 16, 69–76. https://doi.org/10.1097/00004647-199601000-00008.

Mele, T., Jurič, D.M., 2013. Identification and pharmacological characterization of the histamine H_3 receptor in cultured rat astrocytes. Eur. J. Pharmacol. 720, 198–204. https://doi.org/10.1016/j.ejphar.2013.10.028.

Nehlig, A., Coles, J.A., 2007. Cellular pathways of energy metabolism in the brain: is glucose used by neurons or astrocytes? Glia 55, 1238–1250. https://doi.org/10.1002/glia.20376.

Nieto-Alamilla, G., Márquez-Gómez, R., García-Gálvez, A.M., Morales-Figueroa, G.E., Arias-Montaño, J.A., 2016. The histamine H_3 receptor: structure, pharmacology, and function. Mol. Pharmacol. 90, 649–673. https://doi.org/10.1124/mol.116.104752.

Nose, A., Mori, Y., Uchiyama-Tanaka, Y., Kishimoto, N., Maruyamar, K., Matsubara, H., Iwasaka, T., 2003. Regulation of glucose transporter (GLUT1) gene expression by angiotensin II in mesangial cells: involvement of HB-EGF and EGF receptor transactivation. Hypertens. Res. 26, 67–73. https://doi.org/10.1291/hypres.26.67.

Panula, P., Nuutinen, S., 2013. The histaminergic network in the brain: basic organization and role in disease. Nat. Rev. Neurosci. 4, 472–487. https://doi.org/10.1038/nrn3526.

Panula, P., Chazot, P.L., Gutzmer, R., Leurs, R., Liu, W.L., Stark, H., Thurmond, R.L., Haas, H.L., 2015. International union of basic and clinical pharmacology. XCVIII. Histamine receptors. Pharmacol. Rev. 67, 601–655. https://doi.org/10.1124/pr.114.010249.

Pellerin, L., Bouzier-Sore, A.K., Aubert, A., Serres, S., Merle, M., et al., 2007. Activity-dependent regulation of energy metabolism by astrocytes: an update. Glia 55, 1251–1262. https://doi.org/10.1002/glia.20528.

Pini, A., Obara, I., Battell, E., Chazot, P.L., Rosa, A.C., 2016. Histamine in diabetes: is it time to reconsider? Pharmacol. Res. 111, 316–324. https://doi.org/10.1016/j.phrs.2016.06.021.

Prebil, M., Jensen, J., Zorec, R., Kreft, M., 2011. Astrocytes and energy metabolism. Arch. Physiol. Biochem. 117, 64–69. https://doi.org/10.3109/13813455.2010.539616.

Rahman, T., 2012. Dynamic clustering of IP_3 receptors by IP_3. Biochem. Soc. Trans. 40, 325–330. https://doi.org/10.1042/BST20110772.

Rivera-Ramírez, N., Montejo-López, W., López-Méndez, M.C., Guerrero-Hernández, A., Molina-Hernández, A., García-Hernández, U., Arias-Montaño, J.A., 2016. Histamine H_3 receptor activation stimulates calcium mobilization in a subpopulation of rat striatal neurons in primary culture, but not in synaptosomes. Neurochem. Int. 101, 38–47. https://doi.org/10.1016/j.neuint.2016.10.005.

Roskoski, R., 2012. MEK1/2 dual-specificity protein kinases: structure and regulation. Biochem. Biophys. Res. Commun. 417, 5–10. https://doi.org/10.1016/j.bbrc.2011.11.145.

Rozengurt, E., 2007. Mitogenic signaling pathways induced by G protein-coupled receptors. J. Cell. Physiol. 213, 589–602. https://doi.org/10.1002/jcp.21246.

Santalucía, T., Christmann, M., Yacoub, M.H., Brand, N.J., 2003. Hypertrophic agonist induces the binding of c-Fos to an AP-1 site in cardiac myocytes: implications for the expression of GLUT1. Cardiovasc. Res. 59, 639–648. https://doi.org/10.1016/S0008-6363(03)00472-3.

Sim, Y.B., Park, S.H., Kim, S.S., Kim, C.H., Kim, S.J., Lim, S.M., Jung, J.S., Ryu, O.H., Choi, M.G., Suh, H.W., 2014. The modulatory role of spinally located histamine receptors in the regulation of the blood glucose level in D-glucose-fed mice. KOREAN J. PHYSIOL. PHARMACOL. 18, 41–46. https://doi.org/10.4196/kjpp.2014.18.1.41.

Simpson, I.A., Carruthers, A., Vanucci, J.S., 2007. Supply and demand in cerebral energy metabolism: the role of nutrient transport. J. Cereb. Blood Flow Metab. 27, 1766–1791. https://doi.org/10.1038/sj.jcbfm.9600521.

Srinivasan, D., Yen, J.H., Joseph, D., Friedman, W., 2004. Cell type–specific interleukin-1β signaling in the CNS. J. Neurosci. 24, 6482–6488. https://doi.org/10.1523/JNEUROSCI.5712-03.2004.

Steinberg, S.F., 2008. Structural basis of protein kinase C isoform function. Physiol. Rev. 88, 1341–1378. https://doi.org/10.1152/physrev.00034.2007.

Suh, H.N., Han, H.J., 2013. Fibronectin-induced VEGF receptor and calcium channel transactivation stimulate GLUT-1 synthesis and trafficking through PPARγ and TC10 in mouse embryonic stem cells. Stem Cell Res. 10, 371–386. https://doi.org/10.1016/j.scr.2013.01.008.

Tabarean, I.V., 2013. Functional pharmacology of H_1 histamine receptors expressed in mouse preoptic/anterior hypothalamic neurons. Br. J. Pharmacol. 170, 415–425. https://doi.org/10.1111/bph.12286.

Vannier, E., Dinarello, C.A., 1993. Histamine enhances interleukin (IL)-1-induced IL-1 gene expression and protein synthesis via H2 receptors in pheripheral blood mononuclear cells. J. Clin. Investig. 92, 281–287. https://doi.org/10.1172/JCI116562.

Vizcaíno, C., Mansilla, S., Portugal, J., 2015. Sp1 transcription factor: a long-standing target in cancer chemotherapy. Pharmacol. Ther. 152, 111–124. https://doi.org/10.1016/j.pharmthera.2015.05.008.

Xu, J., Zhang, X., Qian, Q., Wang, Y., Dong, H., Li, N., Qian, Y., Jin, W., 2018. Histamine upregulates the expression of histamine receptors and increases the neuroprotective effect of astrocytes. J. Neuroinflammation 15, 41. https://doi.org/10.1186/s12974-018-1068-x.

Yu, S., Ding, W.G., 1998. The 45 kDa form of glucose transporter 1 (GLUT1) is localized in oligodendrocytes and astrocytes but not in microglia in the rat brain. Brain Res. 797, 65–72. https://doi.org/10.1016/S0006-8993(98)00372-2.

Zeng, L., Webster, S.V., Newton, P.M., 2012. The biology of protein kinase C. Adv. Exp. Med. Biol. 740, 639–661. https://doi.org/10.1007/978-94-007-2888-2_28.

Zhao, K., Liu, H.Y., Zhao, F.Q., Liu, J.X., 2014. Protein kinase C regulates glucose uptake and mRNA expression of glucose transporter (GLUT) 1 and GLUT 8 in lactating bovine mammary epithelial cells. J. Dairy Sci. 97, 4329–4332. https://doi.org/10.3168/jds.2013-7848.